Excitation spectrum of Mott shells in optical lattices

Dirk-Sören Lühmann[1], **Kai Bongs**[2] **and Daniela Pfannkuche**[1]

[1] I. Institut für Theoretische Physik, Universität Hamburg, Jungiusstraße 9, 20355 Hamburg, Germany
[2] MUARC, School of Physics and Astronomy, University of Birmingham, Edgbaston, Birmingham B15 2TT, UK

PACS 03.75.Lm – Tunneling, Josephson effect, Bose-Einstein condensates in periodic potentials, solitons, vortices, and topological excitations
PACS 67.85.Hj – Bose-Einstein condensates in optical potentials

Abstract. - We theoretically study the excitation spectrum of confined macroscopic optical lattices in the Mott-insulating limit. For large systems, a fast numerical method is proposed to calculate the ground state filling and excitation energies. We introduce many-particle on-site energies capturing multi-band effects and discuss tunnelling on a perturbative level using an effectively restricted Hilbert space. Results for small one-dimensional lattices obtained by this method are in good agreement with the exact multi-band diagonalization of the Hamiltonian. Spectral properties associated with the formation of regions with constant filling, so-called Mott shells, are investigated and interfaces between the shells with strong particle fluctuations are characterized by gapless local excitations.

Introduction

The equivalence of lattice sites is the foundation of solid state physics as it causes bands and lattice-periodic wave functions. Interesting physics emerges when the band is bend caused by the inhomogeneity of the system, e.g. in clusters, where bulk and surface electrons show a different physical behaviour. In optical lattices, the inhomogeneity comes naturally due to the finite waist of the lattice-establishing laser beams or due to an additional dipole trap. It has been shown in a series of pioneering work [1–3] that the bosonic Mott-insulator phase can be realized in optical lattices. Further measurements [4–6] have demonstrated that the situation is more subtle and Mott-insulator shells appear, i.e. plateaus with constant filling factors descending in integer steps from the centre of the trap. The existence of superfluid regions between the Mott shells has been theoretically predicted [7–12]. The system has previously been studied numerically, using quantum Monte Carlo [7–9] and DMRG [10], and analytically in Refs. [11, 12]. In addition to condensed matter aspects, the coexistence of compressible and incompressible regions has important implications on adiabatic heating in optical lattices [13].

We present a multi-band exact diagonalization study of small systems exploring the exact excitation spectrum and the precursor of shell formation. Based on this calculation we use a numerical method, which in the limit of deep lattices allows us to obtain an approximated energy spectrum and the exact occupation numbers. Thereby, we incorporate orbital changes by introducing a particle-number-dependent on-site interaction. The formation of shells, local excitation gaps and particle fluctuations are discussed reflecting the strong inhomogeneity of the system. Our approach is suitable for optical lattices with millions of atoms in arbitrary spatial dimensions and allows a perturbative treatment of tunnelling. Compared to algorithms such as quantum Monte Carlo [7–9] and DMRG [10], this technique gives numerically inexpensive results for large 3D lattice systems in a specific parameter regime. We organize this paper as follows. Subsequent to the introduction of the system, we present results obtained by means of exact diagonalization followed by the numerical approach for vanishing tunnelling and a comparison of both results. Finally, we discuss consequences for two- and three-dimensional optical lattices including non-zero tunnelling.

The interaction of the ultracold bosonic atoms with mass m is modelled by a contact potential $g\delta(\mathbf{r}-\mathbf{r}')$ with $g=\frac{4\pi\hbar^2}{m}a_s$ and the s-wave scattering length a_s. Using the bosonic field operator $\hat{\psi}(\mathbf{r})$, the Hamiltonian including the repulsive two-particle interaction reads

$$\begin{aligned}\hat{H} &= \int d^3r \left(\hat{\psi}^\dagger(\mathbf{r})\left[\frac{\mathbf{p}^2}{2m}+V_P(\mathbf{r})+V_C(\mathbf{r})\right]\hat{\psi}(\mathbf{r})\right. \\ &\quad \left.+\frac{g}{2}\hat{\psi}^\dagger(\mathbf{r})\hat{\psi}^\dagger(\mathbf{r})\hat{\psi}(\mathbf{r})\hat{\psi}(\mathbf{r})\right), \qquad (1)\end{aligned}$$

where the periodic potential V_P of the optical lattice is given by $V_{0,x}\cos^2(\pi x/a)+V_{0,y}\cos^2(\pi y/a)+V_{0,z}\cos^2(\pi z/a)$ with the lattice constant a. The atoms experience an additional confinement potential V_C caused by the finite Gaussian beam waist W_0 of the laser beams and/or an additional dipole trap with the frequency ω_d. Using a harmonic approach, the confining potential in x-direction is given by

$$V_C = V_h\,\frac{x^2}{a^2}, \qquad (2)$$

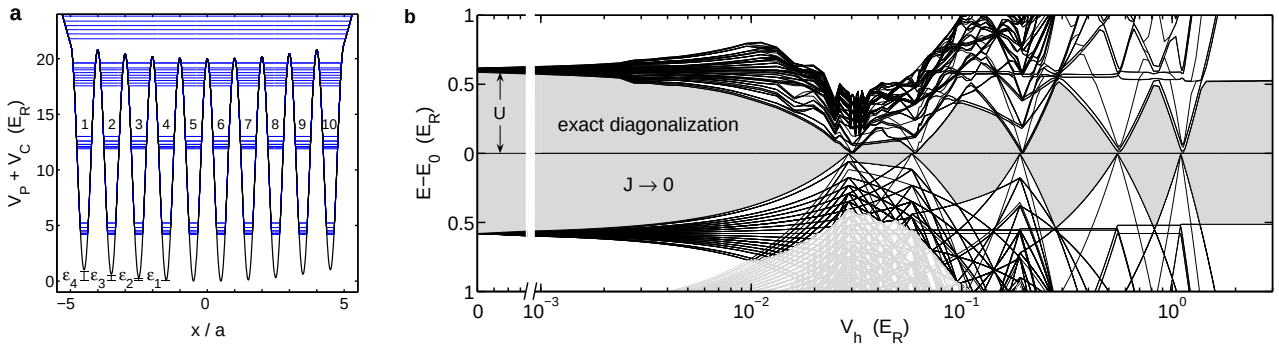

Fig. 1: (a) The periodic potential V_P is superposed by a harmonic potential V_C leading to site offsets ϵ_i. The single-particle spectrum for $V_h = 0.06E_R$ containing discrete bands is plotted within the potential. (b) The many-particle energy spectrum (91 states) obtained by exact diagonalization (upper half) and for vanishing tunnelling (lower half) as a function of the harmonic confinement strength V_h. Additional states in the $J \to 0$ spectrum are plotted in grey. The energy scale is relative to the ground state energy E_0 and the gap to the first excited state is depicted in grey.

where $V_h = \frac{1}{2}m\omega_{\text{eff}}^2 a^2$ with $\omega_{\text{eff}}^2 \approx \frac{4(V_{0,y}+V_{0,z})}{mW_0^2} + \omega_{d,x}^2$.

Exact diagonalization

For the exact diagonalization, the potential is truncated to a 1D lattice with $m_x = 10$ and $m_y = m_z = 1$ sites by adding a smooth boundary [14]. Exemplarily, we have chosen ^{87}Rb atoms with $a_s = 100a_0$, where a_0 is the Bohr radius, $N = 10$ particles, a lattice constant $a = 515$ nm, and a transversal lattice depth $V_{0,y} = V_{0,z} = 40E_R$, where $E_R = \frac{h^2}{8ma^2}$ is the recoil energy. The lattice depth in the longitudinal direction is $V_{0,x} = 20E_R$, leading to a system deep within the Mott-insulator phase for a vanishing harmonic confinement ($V_h = 0$). The potential of the 1D lattice is shown in figure 1a, depicting the energy offsets ϵ_i of the modeled chain, which are labeled $\epsilon_0 = 0$ for the two equivalent central sites and ϵ_4 for the outermost sites. The parabolic shape of the confinement leads to large energy offsets of outer sites, although the offsets are small for central ones. At $V_h = 0$, the single-particle spectrum shows three discrete bands that comprise ten delocalized Bloch states each (corresponding to the number of sites), where the width of the lowest band is $4J \approx 2.4\times10^{-3}E_R$ [15]. For larger values of V_h the 'band' width is given basically by the offset of the outermost sites (see figure 1a). At $V_h \gtrsim 0.4E_R$, the outermost site offset $\epsilon_4 \gtrsim 8E_R$ causes the lowest two single-particle bands to overlap.

To calculate the many-particle spectrum by means of exact diagonalization, we limit the many-particle basis to 500 000 Fock states with lowest energy and freeze out the orbital degrees of freedom in y- and z-direction. Afterwards, we calculate the matrix elements of (1) and obtain the 91 lowest eigenvalues (the ground state and the 90 states of the first band for $V_h \to 0$). The exact diagonalization method includes particle correlations and the admixture of higher bands, i.e., orbital changes taking place for higher fillings [14], but is strongly limited to systems with few lattice sites. The many-particle spectrum is plotted in figure 1b (upper half) relative to the ground state energy E_0 as a function of the harmonic confinement V_h using a logarithmic scale. For convenience, the band gap between the ground state and the first excited state is depicted in grey.

For vanishing confinement ($V_h = 0$), the spectrum shows that the first excited band is gapped from the ground state by the on-site interaction energy of two particles $U \approx 0.6E_R$, which corresponds to the gap of the macroscopic Mott-insulator phase. The atoms are strongly localized on single lattice sites [14], so that all lattice sites are occupied by exactly one particle per site. Increasing the harmonic confinement leads to abrupt crossovers to states with higher integer occupation numbers, i.e. finite size correspondents to Mott shell configurations. In the many-particle spectrum these crossover points are reflected by vanishing energy gaps. In between these points lobe-like energy gaps can be observed, where the lobes correspond to the occupation number configurations 1-1-1-2-2-1-1-1, 1-2-2-2-2-1, 2-3-3-2, 1-4-4-1, and finally for $V_h > 1E_R$ a states with 5 particles on the two central sites [16]. For $V_h < 0.03E_R$, the lattice is commensurately filled with one particle per site. In this region, the excited band broadens with increasing V_h, leading to a slowly decreasing energy gap. At $V_h \approx 0.03E_R$, where the energy gap vanishes, a multitude of low-lying excitations is possible leading to a compressible system. At this point, the double occupation of the central sites, which corresponds to the on-site energy U, becomes energetically preferable to the occupation of the outermost sites with $\epsilon_4 = 20V_h$. Analogous situations exist at the other crossovers, so that the shell structure is dominated by the ratio of on-site interaction $\frac{n_i(n_i-1)}{2}U$ to individual site offsets ϵ_i. The critical behaviour separating different filling configurations manifests itself in the disappearance of the excitation gap.

Classical approach and orbital degrees of freedom

The nature of the excited states, however, is more complicated and the energy spectrum, which contains important physics, is rather complex. In the following, we therefore consider the 'classical' case of vanishing tunnelling ($J \to 0$) which is valid deep within the Mott-insulator phase. Using this approach, we show that the basic features of the spectrum can be uncovered. Furthermore, larger systems can be studied, for which finite tunnelling can be reintroduced perturbatively in a second step,

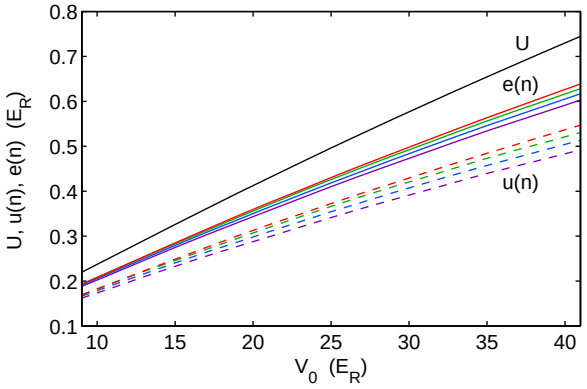

Fig. 2: A comparison of Hubbard on-site interaction U, the many-particle interaction energy $u(n)$, and the total on-site energy $e(n)$ per atom pair for $V_{0,i} = V_0$ and $i = x, y, z$. The single-site many-particle wave function is determined by exact diagonalization for $n = 2$ particles (highest energy) to $n = 5$ particles (lowest energy).

dealing with a drastically reduced basis set. For $J \to 0$, the truncated Bose-Hubbard Hamiltonian is given by

$$\hat{H} = \sum_i \frac{\hat{n}_i(\hat{n}_i - 1)}{2} U + \epsilon_i \hat{n}_i \tag{3}$$

and the localized occupation number basis $|n_1, n_2, ..., n_M\rangle$ is an eigenbasis of the Hamiltonian, where $M = m_x m_y m_z$ denotes the number of sites. In principle, finding the ground state requires to calculate the total energy $E = \langle \hat{H} \rangle$ of all possible basis states. The efficiency of this method is very limited due to the huge number of basis states $\frac{(N+M-1)!}{N!(M-1)!}$ for large lattices, where N is the number of particles. Following [11, 12], in the local density approximation an effective local chemical potential $\tilde{\mu}(\mathbf{r}) = \mu - V_C(\mathbf{r})$ can be introduced, and the ground state is then constructed via filling each lattice site up to the local chemical potential $\tilde{\mu}$ separately. Using the continuous limit, the chemical potential $\mu(N)$ is calculated analytically in [11] and numerically in [12]. The continuous limit is, however, only applicable to smooth confining potentials. In general, the self-consistent determination of $\mu(N)$ is tedious. We therefore suggest the following iterative algorithm for the solution of (3) directly in the microcanonical ensemble with a fixed total particle number $N = \sum_i n_i$. It allows us also to construct the lowest excited states of the system and therefore a comparison with figure 1b (upper half). Starting with an empty lattice, the N particles are added successively to that site j of the lattice, where the expense of energy $\mu_j^+ = n_j U + \epsilon_j$ is presently minimal. This procedure gives the lowest energy occupation for any particle number N, since $\mu_j^+ > 0$ and all sites are uncorrelated. The complexity of this algorithm is given by $O(NM)$, since each step adds one particle to one of M possible sites. This allows the calculation of the exact occupation numbers for a million particles, e.g., $N = M = 100^3$, within seconds on an ordinary desktop computer. This method is therefore considerable useful for the design and interpretation of experiments.

Compared with the exact diagonalization results for the 1D lattice, the crossover points can, in principle, be reproduced with this method but their positions are shifted. This effect is additionally enhanced for higher filling factors. To study this influence more quantitatively, we calculate the on-site few-particle interaction with exact diagonalization. Since the lattice depth is sufficiently deep, it is valid to approximate the lowest-band Wannier function $w_0(\mathbf{r})$ by the wave function of a single sinusoidal lattice site using hard boundary conditions. The correlationless Hubbard on-site interaction $U = g \int d^3r \, |w_0(\mathbf{r})|^4$ does not incorporate that particles tend to avoid each other for repulsive interaction. This causes broadening of the particle density and was addressed experimentally in [5]. Using the correct many-particle wave function Ψ_n for n particles, the expectation value of the on-site interaction becomes

$$u(n) = \frac{g}{n(n-1)} \langle \hat{\psi}^\dagger(\mathbf{r}) \hat{\psi}^\dagger(\mathbf{r}) \hat{\psi}(\mathbf{r}) \hat{\psi}(\mathbf{r}) \rangle, \tag{4}$$

which is normalized to the interaction energy per atom pair. The results that are depicted in figure 2 show that $u(n)$ determined by exact diagonalization deviates strongly from the Hubbard on-site interaction U. As expected, the interaction energy $u(n)$ decreases with an increasing number of particles per site. However, not only $u(n)$ changes when the modification of wavefunctions is taken into account. In fact, the admixture of correlated states and the broadening of the density change the expectation value of on-site kinetic and potential energy. The total on-site energy is the eigenvalue of the many-particle Schrödinger equation $\hat{H}_i \, \Psi_n = E_n \, \Psi_n$ restricted to single-site wave functions and using the full Hamiltonian (1) with $V_h = 0$. The normalized on-site energies $e(n) = 2(E_n - E_n^0)/n(n-1)$ are plotted in figure 2, where E_n^0 is the energy of the non-interacting system. It shows, that the total interaction lies energetically between U and $u(n)$. Nevertheless, the deviation of $e(2)$ from the Hubbard U is large. Using $U = e(2)$, the crossovers are still shifted noticeably for higher fillings (large V_h) comparing with the results for the 1D lattice (upper half of figure 1b). Therefore, we incorporate in our calculations the correct total interaction energy $e(n_j)$ for a single site with the occupation n_j. Please note that the optimization problem remains the same if substituting the energy $\mu_j^+ = n_j U + \epsilon_j$ for adding one particle by $\mu_j^+ = e(n_j+1) - e(n_j) + \epsilon_j$. In the lower half of figure 1b the energy spectrum for vanishing tunnelling ($J \to 0$) is shown using the corrected values of the on-site interaction. In this case, the crossover energies corresponding to the vanishing gaps for $J \to 0$ are in good agreement with the exact diagonalization of the 1D lattice. This result shows, in general, that the introduced filling-dependent on-site interaction $e(n)$ is appropriate to describe effects arising from orbital changes. The small remaining shift of the crossover energies in figure 1b is due to the 'classical' treatment of the states in our approach.

The energy gap can be obtained by removing one particle from site j and adding it to site $k \neq j$. Finding the minimum excitation energy $\Delta E_{j,k}$ for all possible j and k has in general the complexity $O(M^2)$. The excitation energy is given by $\Delta E_{j,k} = \mu_j^+ + \mu_k^-$, where

$$\mu_j^+ = e(n_j + 1) - e(n_j) + \epsilon_j > 0 \tag{5}$$

for adding a particle on site j and

$$\mu_k^- = e(n_k - 1) - e(n_k) - \epsilon_k < 0 \tag{6}$$

for removing a particle from site k. Thus, it is sufficient to minimize μ_j^+ and μ_k^- separately, which reduces the complexity to linear order in M. Finding the next excited state is more complicated, since this state may be an excitation of the ground state but also of the first excited state. For the calculation of the spectrum, a slightly modified Dijkstra algorithm can be used, where one considers the ground state as the node of a graph. This node is expanded according to all possible excitations. Iteratively, the node with the minimum energy, which is not expanded yet, is expanded. Consequently, the list of expanded nodes represents the states with the lowest energy. It is necessary, however, to check whether a created excited state is already a node in the graph, which is a major contribution to the complexity of the Dijkstra algorithm, but can numerically be highly optimized. Using this procedure, the resulting energy spectrum (lower half of figure 1b) reproduces well the basic features, i.e. the band gap, the overall shape and the density of states, of the exact calculation (upper half). Because of interactions, the degeneracy of states is lifted in the exact spectrum, so that the actual energies of many states are shifted.

Macroscopic lattices

Transferring the above results to macroscopic lattices is not straightforward. Enlarging the system's size causes the differences in offset energies of neighbouring sites $\epsilon_j - \epsilon_k$ to decrease substantially when keeping the offset of the outermost sites fixed. This causes the width and the height of the energy lobes in the spectrum to decrease because a huge number of configurations become possible when increasing the number of particles and lattice sites. This process is drastically enhanced in 2D and 3D lattices, where practically the band gap vanishes for all confinement strengths V_h. The only exception is the real Mott-insulator phase, where the outermost sites have an offset smaller than U. In fact, the excitation spectrum of the total system becomes more or less continuous. This might appear contradictory to the insulating property at first glance but the system is inhomogeneous and only some of the atoms can perform gapless excitations. Therefore, local properties are more suited to describe the system, such as particle number fluctuations and the local excitation spectrum. It has already been pointed out [8–11] that the regions with fixed occupation number, the Mott-insulator shells, are surrounded by compressible shells for non-negligible tunnelling.

Exemplarily, the occupation number distribution n_i for $N = 10^6$ particles in a 3D lattice is depicted in figure 3a. It shows the expected shell structure with filling factors five (in the centre) to one. An advantage of the presented numerical algorithm is that it is also applicable to rapidly varying confinement potentials. It can thus be used to tailor more sophisticated shell configurations for experiments. Since the on-site interaction energy U is relatively small compared to the depth of the lattice wells, the local filling factors can be adjusted without a stronger perturbation of the 3D lattice. Additional laser beams or magnetic fields can thus be used to obtain complex spatial distributions

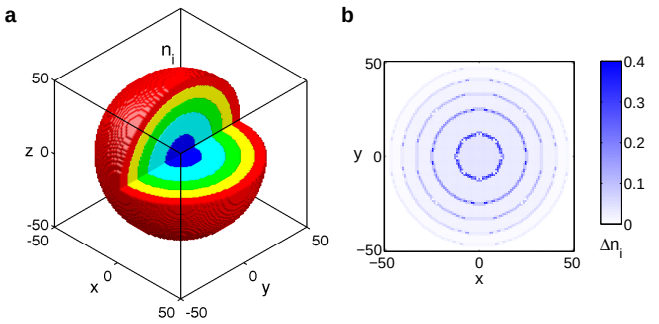

Fig. 3: (a) Cut through the occupation number distribution n_i of a 3D lattice ($N = 10^6$, $J = 0$, $V_h = 7.5 \times 10^{-4} E_R$ and $V_0 = 25 E_R$) showing fillings $n_i = 1$ (outer shell) to $n_i = 5$ (inner shell). (b) Particle fluctuations Δn_i due to finite tunnelling ($J = 10^{-3} E_R \approx 2 \times 10^{-3} U$) appear at the surfaces of the shells ($z = 0$ plane).

of atoms with specific filling factors. Figure 4a shows the occupation number distribution for an added periodic potential in x-direction $V_C = V_h x^2/a^2 + U \cos^2(\pi x/a')$ with the periodicity $a' = 3a$ motivated by [17]. The superlattice structure leads to alternating local fillings. As a second example, an added hat-shaped ($-|x|$) potential causes two separate atomic clouds, shown in figure 4b, that are in touch with each other at the origin.

Single particle excitations and finite tunnelling

At the outer surface of each shell, almost gapless excitations are possible via the hopping of a particle to another site, whereas the inner surface can easily absorb particles. This is shown quantitatively in figure 5a (upper half), where $\Delta E_i^- = \mu_i^- + \min_j(\mu_j^+)$ is the minimal energy for removing one particle from site i and adding it to another site j. The minimal energy for adding one particle to site i (and removing it from site j) is denoted as $\Delta E_i^+ = \mu_i^+ + \min_j(\mu_j^-)$ (lower half of figure 5a). The local excitation gap vanishes at the outer and inner surfaces and increases strongly within the shells. The excitation energies $\Delta E_i^\pm$ are explicitly shown for sites with $y = z = 0$ in figure 5b. It reflects basically the harmonic shape of the confinement, so that ΔE_i^+ and ΔE_i^- are positive and negative parables, respectively, subtracted by integer multiples of the on-site interaction. The situation changes drastically, if accounting only for excitations to nearest neighbours as shown in figures 5c and 5d. Low energy excitations (either ΔE_i^+ or ΔE_i^-) can occur exclusively on sites directly at the boundary between different shells. Within the bulk the single-particle excitation gap is wide and nearly constant. Therefore, the nearest-neighbour tunnelling is, in general, strongly suppressed on these sites, where the system is a good insulator.

In the following, we use a perturbative approach to obtain particle fluctuations for finite tunnelling J. For each site i the subsystem containing the site i and all neighbouring sites is considered. The diagonalization of this subsystem with finite tunnelling $-J \sum_{\langle i,j \rangle} \hat{b}_i^\dagger \hat{b}_j$ allows an approximative calculation of the particle fluctuations $\Delta n_i = \sqrt{\langle \hat{n}_i^2 \rangle - \langle \hat{n}_i \rangle^2}$. For the example above, weak tunnelling causes finite fluctuations Δn_i at the boundaries of the shells, which is shown in figures 3b and

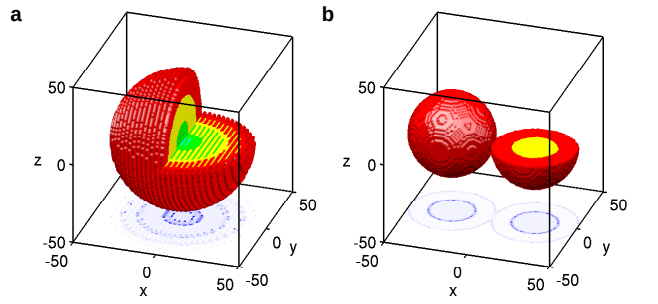

Fig. 4: (a) An additional standing wave with periodicity $3a$ and amplitude U causes alternating fillings in x direction ($N = 3.5 \times 10^5$). (b) An added $-50V_h|x|$ potential leads to two separate atom spheres ($N = 1.5 \times 10^5$). The fluctuations Δn_i for $J = 10^{-3}E_R$ and $z = 0$ are shown at the bottom (see figure 3 for the colour map and other parameters).

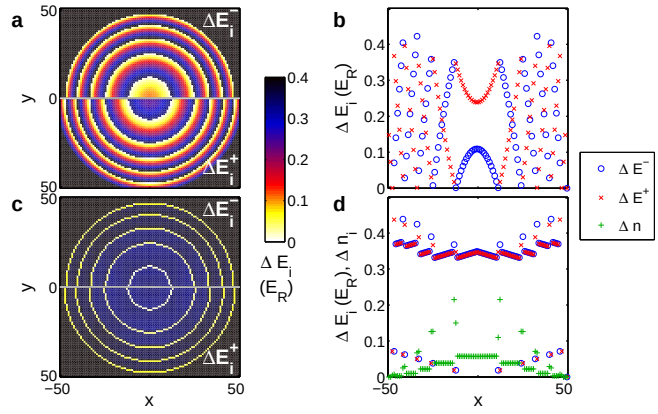

Fig. 5: The minimal excitation energy in the $z = 0$ plane (a) and for $y = z = 0$ (b) for particles hopping from site i (E_i^-) and to site i (E_i^+). The excitation energies only accounting for nearest-neighbour hopping in the $z = 0$ plane (c) and for $y = z = 0$ (d) including particle fluctuations Δn_i for $J = 5 \times 10^{-3}E_R$.

4 for $J = 10^{-3}E_R$ and in figure 5d for $J = 5 \times 10^{-3}E_R$. Please note, that due to the finite cell size of the lattice, the results are not completely spherically symmetric. In accordance with the nearest-neighbour excitation energies, the fluctuations affect only sites directly at the surfaces. Because of the larger slope of the confinement and the lower filling, the tunnelling decreases for outer shells. Within the bulk of the Mott shells small particle fluctuations can be observed due to the finite tunnelling. The fluctuations on the surface however enhance the tunnelling of atoms next to the surface, which is not covered by this perturbative approach and would require a self-consistent calculation. The narrow energy gaps of particles close to the surface can, in principle, cause near-resonant tunnelling to non-nearest neighbours, so-called variable range hopping [18]. Due to the relatively strong V_h (compared with J) and the regularity of the potential, only sites on the surface, which are dominated by nearest-neighbour hopping, have suitably low excitation energies.

The presented method provides the lowest energetic states (including particle-hole excitations) and is suitable to restrict the Hilbert space effectively. The obtained states can be used as a starting point for exact diagonalization, quantum Monte-Carlo, and dynamical mean-field calculations including tunnelling and finite temperatures. In particular, the diagonalization of the 1D lattice (figure 1b) could be transformed with much fewer basis states.

Conclusions

In summary, we have studied the excitation spectrum and exact site occupation numbers for confined optical lattices deep within the Mott insulator regime. In good agreement with exact diagonalization for small 1D lattices, a numerical method was presented that allows for negligible tunnelling the exact treatment of macroscopic optical lattices with arbitrary shape of the confining potential. Adding slowly varying potentials to the optical lattice can give rise to complex filling structures. We have calculated the numerically exact many-particle on-site energies and have shown that introducing a filling factor depending on-site interaction can be incorporated to cover orbital changes. For small systems, the many-particle spectrum contains lobes, whereas for macroscopic systems nearly gapless excitations are always possible at the boundaries of the Mott shells. Within a given Mott shell the local excitation energy varies strongly leading to compressible sites close to the surface and incompressible inner sites. A perturbative treatment for finite tunnelling shows strong particle fluctuations at the boundaries between the shells, where the Mott-insulator gap vanishes. Finally, the presented method can serve as a reduction scheme for the Hilbert space for further numerical treatments.

Acknowledgments

We would like to thank P. Ernst and K. Sengstock for valuable discussions.

REFERENCES

[1] D. Jaksch, C. Bruder, J. I. Cirac, C. W. Gardiner, and P. Zoller, Phys. Rev. Lett. **81**, 3108 (1998).
[2] M. Greiner, O. Mandel, T. Esslinger, T. W. Hänsch, and I. Bloch, Nature (London) **415**, 39 (2002).
[3] T. Stöferle, H. Moritz, C. Schori, M. Köhl, and T. Esslinger, Phys. Rev. Lett. **92**, 130403 (2004).
[4] S. Fölling, A. Widera, T. Müller, F. Gerbier, and I. Bloch, Phys. Rev. Lett. **97**, 060403 (2006).
[5] G. K. Campbell, J. Mun, M. Boyd, P. Medley, A. E. Leanhardt, L. G. Marcassa, D. E. Pritchard, and W. Ketterle, Science **313**, 649 (2006).
[6] P. Cheinet, S. Trotzky, M. Feld, U. Schnorrberger, M. Moreno-Cardoner, S. Fölling, and I. Bloch, Phys. Rev. Lett. **101**, 090404 (2008).
[7] G. G. Batrouni, V. Rousseau, R. T. Scalettar, M. Rigol, A. Muramatsu, P. J. H. Denteneer, and M. Troyer, Phys. Rev. Lett. **89**, 117203 (2002).
[8] V. A. Kashurnikov, N. V. Prokof'ev, and B. V. Svistunov, Phys. Rev. A **66**, 031601(R) (2002).
[9] S. Wessel, F. Alet, M. Troyer, and G. G. Batrouni, Phys. Rev. A **70**, 053615 (2004).
[10] C. Kollath, U. Schollwöck, J. von Delft, and W. Zwerger, Phys. Rev. A **69**, 031601(R) (2004).
[11] B. DeMarco, C. Lannert, S. Vishveshwara, and T.-C. Wei, Phy. Rev. A **71**, 063601 (2005).

[12] F. Gerbier, A. Widera, S. Fölling, O. Mandel, T. Gericke, and I. Bloch, Phys. Rev. A **72**, 053606 (2005).
[13] T.-L. Ho and Q. Zhou, Phys. Rev. Lett. **99**, 120404 (2007).
[14] D.-S. Lühmann, K. Bongs, K. Sengstock, and D. Pfannkuche, Phys. Rev. A **77**, 023620 (2008).
[15] Due to the symmetry of the potential, the two lowest bands contain nearly degenerate symmetric and antisymmetric states localized on two equivalent sites.
[16] For certain system parameters (N, m_x, V_h) a degeneracy of the ground state can occur.
[17] S. Peil, J. V. Porto, B. Laburthe Tolra, J. M. Obrecht, B. E. King, M. Subbotin, S. L. Rolston, and W. D. Phillips, Phys. Rev. A **67**, 051603(R) (2003).
[18] V. Ambegaokar, B. I. Halperin, and J. S. Langer, Phys. Rev. B **4**, 2612 (1971).